

GENERATING 3D MODELS FROM BIOMEDICAL IMAGES VIA VOLUMETRIC SEGMENTATION

S Sowmiya Sree - 2018103598 - sowmiponni05@gmail.com

S Juanita - 2018103544 - nitajuja@gmail.com

ABSTRACT

The prime idea is to generate a workflow that can convert volumetric medical imaging data (MRI and CT images) to 3D models. This would have several uses, and promoting patient education is also one of our main goals. Our work focuses on implementing advanced segmentation algorithms capable of detecting smaller structures and separating boundary regions precisely, then producing 3D models capable of 3D printing. The segmentation yielded good results because reliable models were transported for mesh refinement and 3D modeling.

1 INTRODUCTION

Anatomical models are essential training and teaching tools in the clinical environment and are routinely used in medical imaging research. Medical image segmentation plays a pivotal role in computer-aided diagnosis systems, which help make clinical decisions. Segmenting a region of interest like an organ or lesion from a medical image or a scan is critical. It contains details like the volume, shape, and location of the region of interest. Automatic methods proposed for medical image segmentation help radiologists make fast and labor-less annotations. Early methods were based on traditional pattern recognition techniques like statistical modeling and edge detection filters. Later, machine learning approaches using hand-crafted features based on the modality and type of segmentation task were developed. Recently, the state-of-the-art methods for medical image segmentation for most modalities like magnetic resonance imaging (MRI), computed tomography (CT), and ultrasound (US) are based on deep learning. As convolutional neural networks (CNNs) extract data-specific features rich in quality and effective in representing the image and the region of interest, deep learning reduces the hassle of extracting manual features from the image. Advances in segmentation algorithms and the increased availability of three-dimensional (3D) printers have made it possible to create cost-efficient patient-specific models without expert knowledge. The prime idea is to generate a workflow that can convert volumetric medical imaging data (MRI and CT images) to 3D models. Our work focuses on implementing advanced segmentation algorithms capable of detecting smaller structures and separating boundary regions precisely (patient-specific). We propose a convolutional architecture for volumetric segmentation. The volumetric segmentation is followed by mesh refinement, which focuses on repairing, smoothing, and appending with other related segments. This post-processing of the segments is expected to generate clean deliverables for 3D model generation. Software like Autodesk Meshmixer can refine and visualize the 3D models. The core intention is to build efficient image segmentation architecture which serves as the backbone for the entire workflow.

The previous works on the field of 3d biomedical images, i.e., scan segmentation and 3d object modeling, are widely described in [2]. Next, the data used for the project is thoroughly examined in [3]. This is then followed by a detailed explanation of the segmentation architecture along with its components in [4]. Having talked about the backbone of architecture for volumetric segmentation, the results obtained from segmentation as well as mesh refinement and final results are displayed in [5]. The obtained results are analyzed in detail [6].

2 RELATED WORK

The segmentation of biomedical images has been a topic of great interest since the past. Parallely, there also have been works for modeling 3D objects. Seg-Net [1] was the first such type of network that was widely recognized. In the encoder block of Seg-Net, every convolutional layer is followed by a max-pooling layer which causes the input image to be projected onto a lower dimension similar to an under complete auto-encoder. The receptive field size of the filters increases with the depth of the network, thereby enabling it to extract high-level features in the deeper layers. The initial layers of the encoder extract low-level information like edges and small anatomical structures. In contrast, the deeper layers extract high-level information like objects (in the case of vision datasets) and organs/lesions (in the case of medical imaging datasets). A breakthrough in medical image segmentation was brought by U-Net [2] where skip connections were introduced between the encoder and decoder to improve the training and quality of the features used in predicting the segmentation. U-Net has become the backbone of almost all the leading methods for medical image segmentation in recent years. Subsequently, many more networks were proposed, built on top of U-Net architectures. The U-Net++ proposed using nested and dense skip connections for further reducing the semantic gap between the feature maps of the encoder and decoder. The UNet3+ proposed using full-scale skip connections where skip connections are made between different scales. 3D U-Net [3] and V-Net [4] were proposed as extensions of U-Net for volumetric segmentation in 3D medical scans. The main problem with the above family of networks is that they lack focus in extracting features to segment small structures. More high-level features get extracted as the networks are built to be more profound. Even though the skip connections facilitate the transmission of local features to the decoder, from our experiments, we observed that they still fail at segmenting small anatomical landmarks with blurred boundaries. Although U-Net and its variants are good at segmenting large structures, they fail when the segmentation masks are small or have noisy boundaries. The U-Net 3D was unable to capture the low-level features in the 3D image.

On the contrary, Kite-Net 3D was good at capturing the low-level features but couldn't retain the overall shapes of the provided image. Hence, both of these architectures were combined to produce over-complete convolutional architecture KiU-Net 3D [5]. Delving into the 3D modeling part, the publication by a group of radiologists in America [6] talked about the emerging future of 3D printing in the medical/surgical field. Yet another publication by a group of medical researchers [8] talks about the replacement of reconstructing the 3D vessel geometry from computed tomography patient scans with the 3D printing to produce phantoms. The detailed procedures involved in transforming the volumetric images to efficient 3D print models are thoroughly investigated in [9].

3 SOURCE DATA

The BraTS dataset provided by the “Center for Biomedical Image Computing Analytics” of the “Perlman school of medicine” is chosen. The dataset is used for Multimodal Brain Tumor Segmentation. The dataset consists of 335 MRI scans with each scan having 155 slices (each of 255*255 dimension). For the brain tumor classification task, 4 classes of tumors are provided namely

1. Enhancing Tumor
2. Peritumoural edema
3. Necrotic
4. Non enhancing Tumor

The 2020 version of the BraTS was chosen for the project. It consists of 2 folders for testing and validation. Each folder comprises of scans for a single patient in each subfolder. Each subfolder has the input MRI scan in 3 contrasts namely,

- **T1** - The list of entities associated with a high signal intensity on T1-weighted images is extensive and classically includes fat, proteins, hemorrhage, melanin and gadolinium.
- **T1ce** - The T1 scan with enhanced contrast
- **T2** - T2 reflects the length of time it takes for the MR signal to decay in the transverse plane. A short T2 means that the signal decays very rapidly. So substances with short T2's have smaller signals and appear darker than substances with longer T2 values.
- **Flair** - Fluid-attenuated inversion recovery (FLAIR) is a magnetic resonance imaging (MRI) sequence that produces strong T2 weighting, suppresses the CSF signal, and minimizes contrast between gray matter and white matter.

It is also important to note that the testing folder consists of the ground truth segmented tumor files and the input contrast images. The Validation folder doesn't have these ground truth images for evaluation purposes.

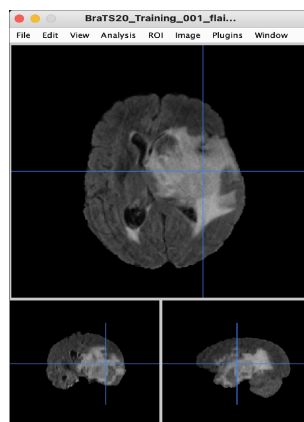


Figure 1 : The input scan viewed in Mango software

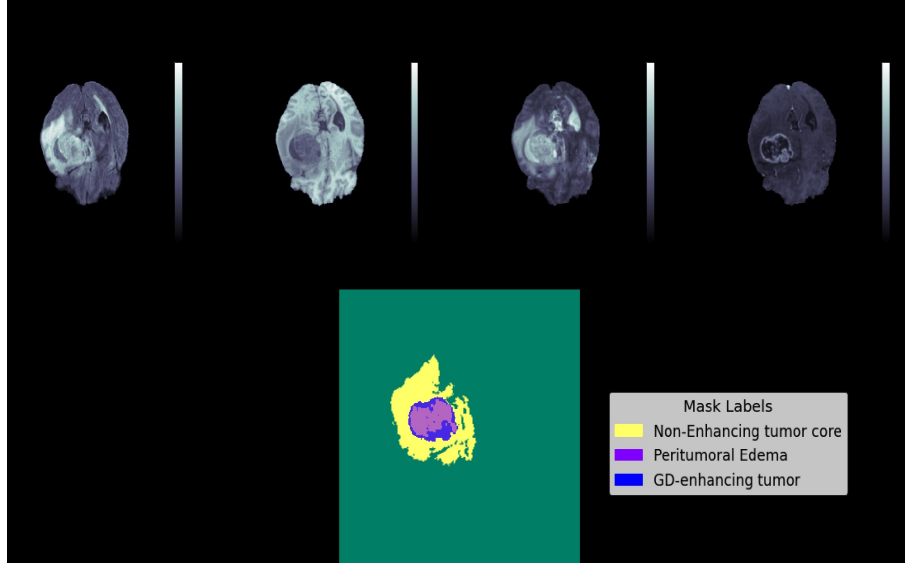


Figure 2 : The input scan of a single patient in all contrasts along with varying classes of tumor

4 SYSTEM DESIGN

The complete architecture diagram is given below. As stated above, the 3d print model is done in three main stages, 1. Volumetric segmentation, 2. Mesh refinement and 3. Generating 3D print model. This section talks about each of these stages in detail.

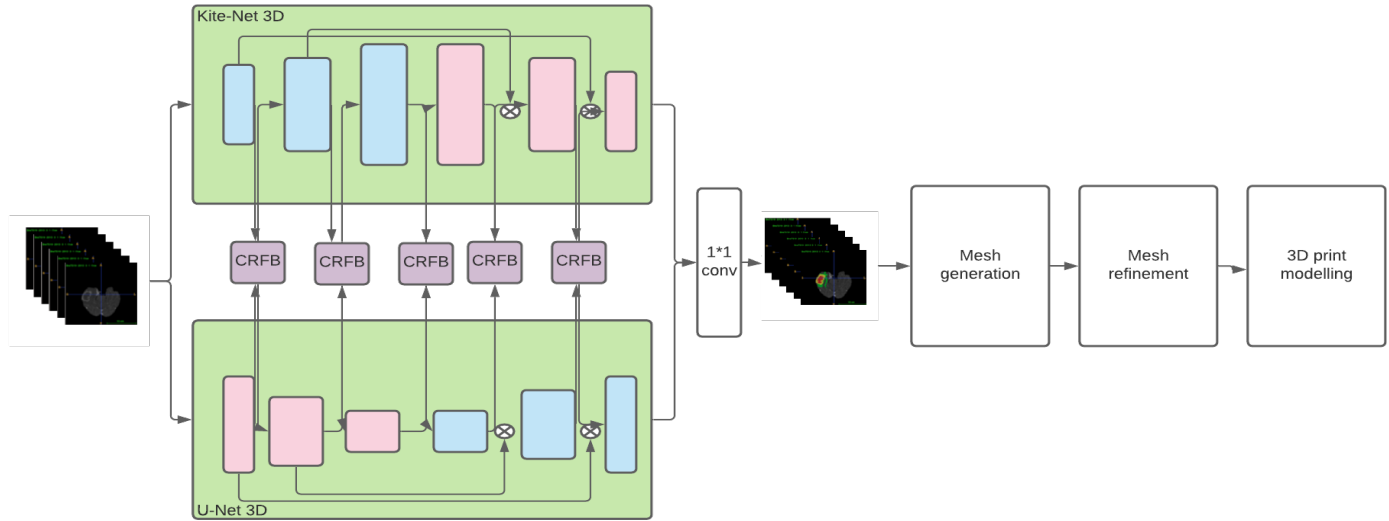


Figure 3 : Complete architecture of the proposed system

4.1 VOLUMETRIC IMAGE SEGMENTATION

This section describes the architecture utilized for the segmentation of 3D scans. The core architecture

chosen for the segmentation is the KiU-Net. The Inputs, process involved and the output generated are given as follows.

4.1.1 IPO

Input : 3D MRI (Brain) and CT (Liver) scans

Process : The input scans in voxel space are initially preprocessed and fed into the devised CNN model. The model is split into 4 major components namely,

- **Kite-Net 3D** - Tan over complete convolutional network which learns to capture fine details and accurate edges of the input.
- **U-Net 3D** - for learning high level features.
- **CRFB (Cross Residual Fusion Block)** - residual features of Kite-Net 3D are learned and added to the features of U-Net 3D to forward the complementary features to U-Net and vice-versa.
- **1*1 3D Convolutio** - The feature maps from last layer of both the branches (Kite-Net 3D and U-Net 3D) are added and passed into this 1*1 3D convolutional layer to get the prediction.

Output : Raw 3D segments

4.1.2 Comaprison of architectures

Before explaining the components and functionality of the proposed architecture, we also describe the base architectures like U-Net and Kite-net, the drawbacks and how combining these two architectures can elevate the segmentation performance.

U-Net 3D

The network consists of contracting and expansive paths, giving it the u-shaped architecture. The contracting path is a typical convolutional network that consists of repeated convolutions, each followed by a rectified linear unit (ReLU) and a max-pooling operation. During the contraction, the spatial information is reduced while feature information is increased. The expansive pathway combines the feature and spatial data through a sequence of up-convolutions and concatenations with high-resolution features from the contracting path. The visual representation of the image is given in Figure 3.

Drawbacks -Experiments suggest that these methods fail to detect tiny structures in most cases. This does not cause much decrement in terms of the overall dice accuracy for the prediction since the datasets predominantly contain images with large structures. However, it is crucial to detect tiny structures with high precision since it plays a vital role in diagnosis. Furthermore, even for the large structures, U-Net-based methods result in erroneous boundaries, especially when the edges are blurry.

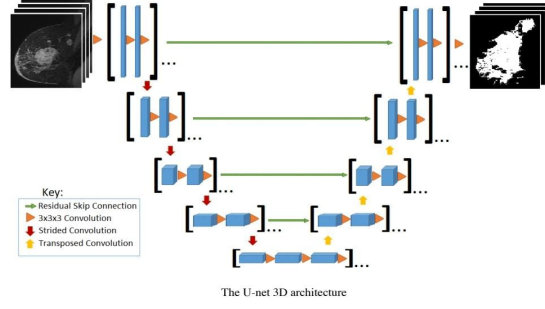


Figure 4 : U-Net 3D

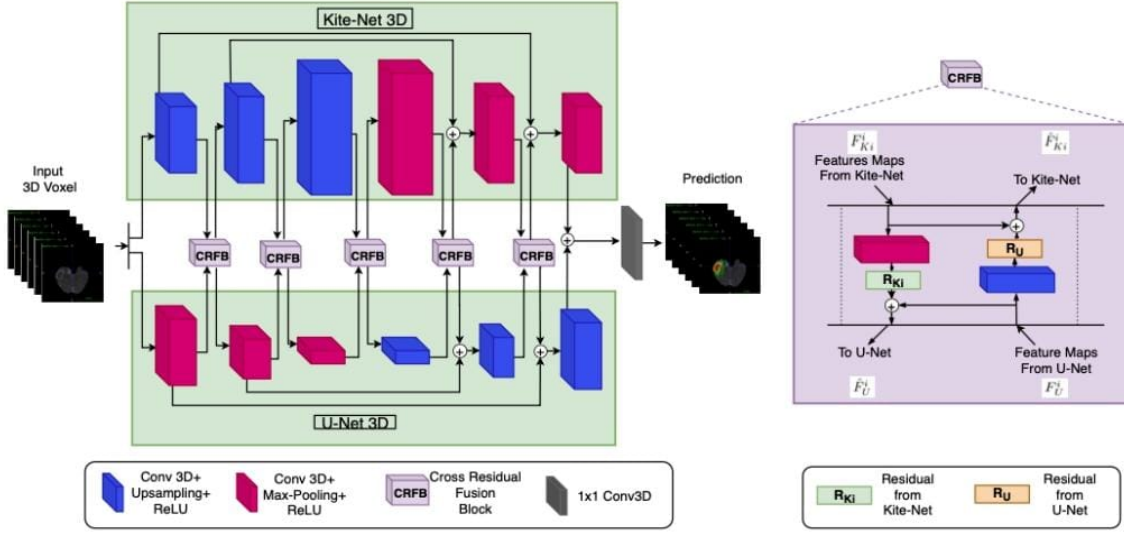
Kite-Net 3D

Kite-Net learns low-level features better than U-Net, it does not learn any high-level features. Due to this, Kite-Net is unable to segment out any large masks present in the input image. To overcome this, we propose KiU-Net 3D, which efficiently combines both Kite-Net and U-Net 3D while achieving the best of both networks.

KiU-Net 3D : U-Net 3D and Kite-Net combined

KiU-Net is a two-branch network where one branch is Kite-Net and the other is U-Net 3D. This network exploits the low-level fine edge capturing the power of Kite-Net 3D and the high-level shape capturing the power of U-Net 3D. The input image is forwarded to Kite-Net 3D and U-Net 3D in parallel. In the encoder of the Kite-Net 3D branch, every convolution block has a convolution 3D layer followed by a trilinear up-sampling layer with the coefficient of two and ReLU activation. In decoder, every convolution block has a convolution 3D layer followed by a 3D max-pooling layer with two and ReLU activation coefficient. Similarly, in the encoder of the U-Net 3D branch, every convolution block has a convolution 3D layer followed by a 3D max-pooling layer with a coefficient of two and ReLU activation. Every convolution block has a convolution 3D layer in the decoder, followed by a trilinear upsampling layer with two and ReLU activation coefficients. The visual representation of the architecture is shown in figure 4.

CRFB - In order to further exploit the capacity of the two networks, we propose to combine the features of the two networks at multiple scales through a novel cross residual feature block (CRFB). That is, at each level in the encoder and decoder of KiU-Net 3D, we combine the respective features using a CRFB. As we know that the features learned by U-Net 3D and Kite-Net 3D are different from each other, this characteristic can be used to further improve the training of the individual networks. So, we try to learn the complementary features from both the networks which will further improve the quality of features learned by the individual networks.



The proposed model i.e., KiU-Net 3D

Figure 5 : KiU-Net 3D and CRFB

4.2 MESH REFINEMENT

The segmented brain tumor was refined using Meshmixer to improve its topology. This was done by adjusting the mesh density of the surface and by applying a global smoothing filter that removes step artifacts due to the finite voxel size. Furthermore, we have used Free-CAD to design a holder for a tissue phantom. FreeCAD has limitations working with large mesh files; the holder was attached to the tumor structure in another software package called Blender. The tumor model was also smoothed using MeshMixer. The different segmentation methods demanded a local smoothing approach utilizing the “RobustSmooth” brush provided by the software. Furthermore, the “Flatten” and “Inflate” brushes were used to remove unphysiological holes in the model. The smoothing of the tumor was also done utilizing both a global smoothing filter and the “RobustSmooth” brush tool.

4.2.1 IPO

Input : Extracted segments (from input scans)

Process : The raw segments are fine tuned and mesh refined so that the segments are error-free in the 3D printing software’s (Cura) environment. Apart from resolving errors, additional preprocessing are essential for rendering accurate 3D models. The prime tasks involves are,

- **Reapiring** - Errors and discontinuities that arise in the image segmentation and exporting process are repaired.
- **Smoothing** - Smoothing the surface of the mesh model to further mitigate the stair-casing error

resulting from the resolution of original medical image.

- **Appending** - Combine all the necessary segments and removing unneeded parts from segmentation.

Output : Mesh refined segments capable of 3D model generation

4.3 3D PRINT MODEL GENERATION

The final yet most defining part of the project is the 3D model generation. The procedures are carried out in the "Cura" software. Customizing the print material and deciding the infill percentage of the 3D mesh files are some of the procedures done in this module. The series of processes involved in defining and customizing the imported mesh, which is then transformed into a 3D model is Making minor corrections in the cleaned mesh file, Customizing the layer height, Adjusting the thickness of the object (top, bottom, left, right), Providing the infill percentage for portions of the 3D model and Deciding the required print material. The software provides several other advanced options. But we restrict ourselves to these procedures since they are sufficient to get decent 3D models. Due to the high cost of 3D printers and options for printing, we visualize the model in the software. But this can be extended easily if resources are available.

4.3.1 IPO

Input : Mesh refined models

Process : The mesh refined models are processed thoroughly and rendered to produce models for 2 main purposes as follows,

- **Segment analyzation** - The segmented portion from the scan i.e., Tumor from brain scans and lesion from liver scans are rendered with intrinsic features capable of examination by surgeons. The torch tensor is converted into 3D numoy array after which it's converted into a mesh file. This is followed by mesh refinement and transferring it to the 3D print software environment
- **Segment localisation** - The identified segment is projected with along with its organ to precisely locate the defect. This involves combining the predicted segment along with the input file. When this stacked 3D array is visualized in softwares, the location of the tumor is clearly visible and this component is patient specific i.e., the location and tendency of tumors varies with patients.

Output : Final 3D models ready to be deployed for 3D printing, intrinsic evaluation (surgeons anatomy students)

5 EXPERIMENTAL RESULTS

The results of the volumetric segmentation is measured in terms of two specific metrics namely, dice and Jaaccard metrics and the conventional accuracy as well.

Dice coefficient (DICE) - 2 * the Area of Overlap divided by the total number of pixels in both images. Also called the overlap index, is the most used metric in validating medical volume segmentations.

$$DICE = \frac{2|(S_g)^1 \cup (S_t)^1|}{|(S_g)^1 + (S_t)^1|} = \frac{2TP}{2TP + FP + FN} \quad (1)$$

Jaccard (JAC) - The Intersection over Union (IoU) metric, is essentially a method to quantify the percent overlap between the target mask and our prediction output. This metric is closely related to the Dice coefficient which is often used as a loss function during training.

$$JAC = \frac{|(S_g)^1 \cap (S_t)^1|}{|(S_g)^1 \cup (S_t)^1|} = \frac{TP}{2TP + FP + FN} \quad (2)$$

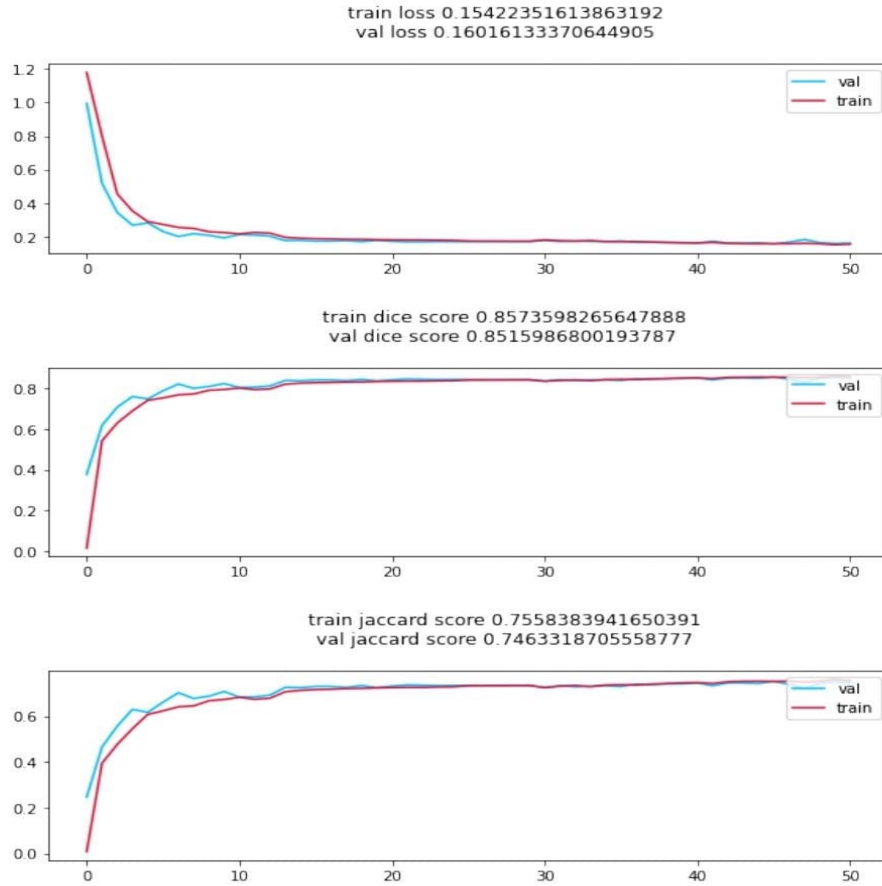


Figure 6 : The plots of 3 metrics to evaluate the model

The ability of the model is evaluated still further by analysing how far it can evaluate the varying types of tumor. The accuracies are good enough to prove that the model segments the tumors very well.

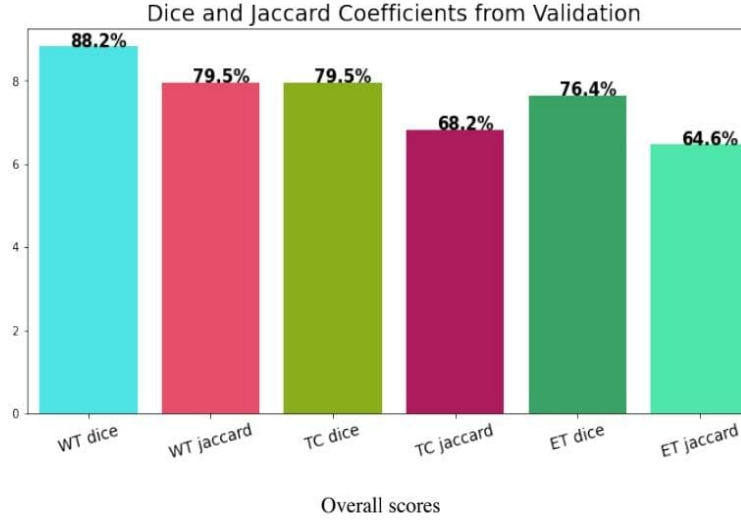


Figure 7 : The model's score in segmenting specific classes of tumor

6 RESULT ANALYSIS

The results obtained from each section is thoroughly examined as shown below. First we have the segments of tumor from the input scan visualized in a 3d gif format. The figure 7 shows that the proposed model segments the region of interest very well. The ground truth segment is the file given in the dataset, whereas the prediction comes from the segmentation architecture.

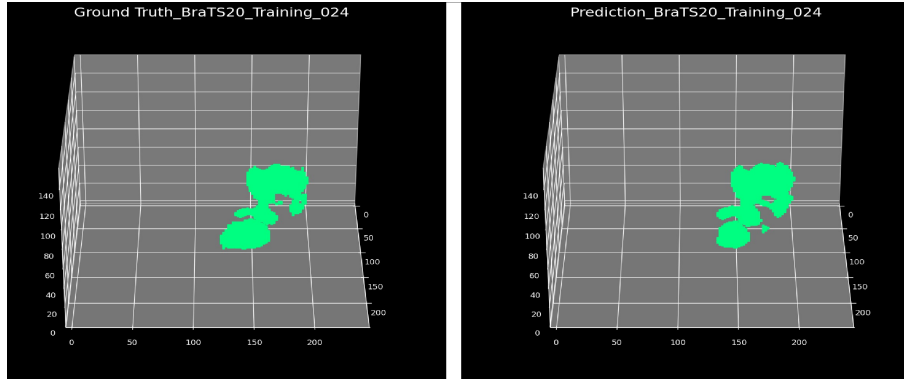


Figure 8 : segmented tumor in comparison with ground truth segment

Having analysed the segments' accuracy, we generate mesh files in ".stl" format and export them to the software Autodesk MeshMixer. There the mesh file is smoothened using various tools and made error free in the 3D environment.

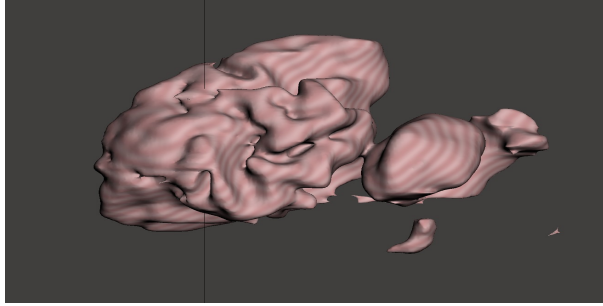


Figure 9 : The processed mesh of a sample segmented tumor

Also as an additional component of innovation, we made it possible to not just analyze the tumor but also to locate the tumor in the brain as shown in figure 9 below.

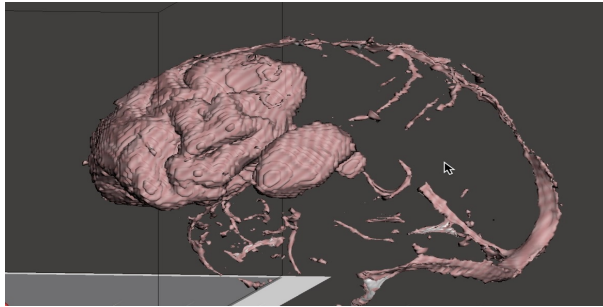
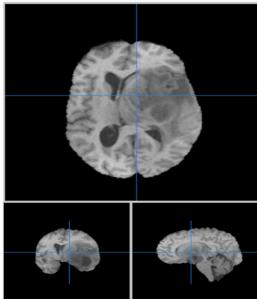
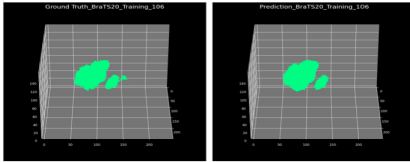
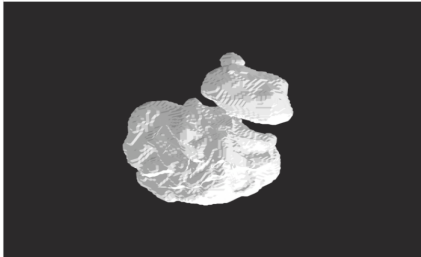
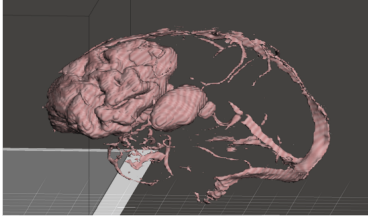
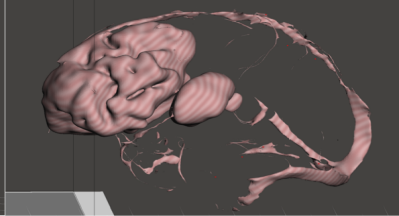
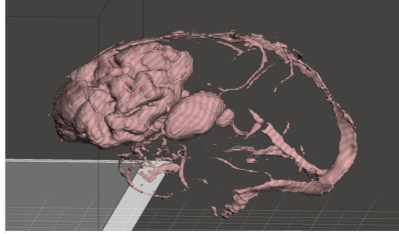


Figure 10 : The processed mesh of a sample segmented tumor

6.1 TABULATING THE USE CASES AND OUTPUTS

| Test case | Input MRI Scan | Expected output vs Predicted output |
|--------------------|---|--|
| Tumor segmentation |  |  |
| Mesh Generation | <p>The torch tenso which is to be converted into 3D numpy array which is then converted into “stl” file I.e., mesh object.</p> |  |

| Test case | Input (mesh in Autodesk) | output (mesh object refined) |
|--------------------------------|--|--|
| Mesh Refinement |  |  |
| Locating the position of tumor | 3D Numpy array converted from the tensor and the predicted segment & input file combined |  |

7 CONCLUSION

The task of Generating 3D models from the biomedical images via volumetric segmentation was split into three main modules, out of which the first module, i.e., “The brain tumor segmentation,” was the backbone. The Brain scans of all four contrasts were stacked for accurate segmentation employing the overcomplete “KiU-Net 3D,” which best utilizes the peculiar aspects of “Kite-Net 3D” and “U-Net 3D”. The main motive of the project was to generate 3D models from precisely segmented brain tumors for doctors to scrutinize and for the study purposes of anatomical students. The proposed segmentation architecture has segmented tumors very well, not just as a whole but also every class of tumor with decent accuracy, shown in figure 6. The architecture is complex enough and consumes an average of 20 mins for every epoch, and 30 epochs have been implemented. The results have come out well with decent DICE and JAC scores, as given in the “Experimental results” section. Further, the model’s capability was displayed with the scores of segmenting all three classes of tumors which is quite impressive. This was then followed by Mesh generation and refinement of the generated meshes. Repairing, smoothing, and making the mesh error-free were the prime motive of the module. It’s crucial to transform a simple mesh file into proper error-free and usable 3D mesh, which could be imported into the 3D software environment for further use. Also, the 3d model formation from the segmented tumors gives purpose and meaning to the segmentation. They have been implemented in licensed software and processed to the maximum extent. As a component of innovation, we incorporated an additional deliverable locating the tumor in the input brain, which is coded patient-specific.

The details of this innovation were well explained in the above sections and visualized as a mesh file in Autodesk Meshmixer. Though helpful for doctors, this feature is perfect for promoting patient education. Finally, these models were incorporated into the Cura software, and mesh files were transformed into 3D models.

8 FUTURE WORKS

As mentioned earlier, the project has focused on precise volumetric segmentation and further developing 3D models for many purposes. One potential future work direction could be focusing on memory-efficient segmentation architecture, resulting in better segmented tumors and faster execution of the CNN model. We have shown that the model segments the tumors from the brain and segments every class of tumor very well. So this can be extended to pigment each of these classes, combined them, and then transform this combined tumor into the software for 3D modeling. This could further aid for better analysis for the surgeons. The next possible area of exploration is the 3D modeling techniques. We have tried the basic techniques. If enough resources are available to afford the 3D printer, other perfections would be needed to get perfect 3D printed models.

References

- [1] V. Badrinarayanan, A. Kendall, and R. Cipolla, “Segnet: A deep convolutional encoder-decoder architecture for image segmentation,” *IEEE transactions on pattern analysis and machine intelligence*, vol. 39, no. 12, pp. 2481–2495, 2017.
- [2] O. Ronneberger, P. Fischer, and T. Brox, “U-net: Convolutional networks for biomedical image segmentation,” in *International Conference on Medical image computing and computer-assisted intervention*, pp. 234–241, Springer, 2015.
- [3] O. C. İcik, A. Abdulkadir, S. S. Lienkamp, T. Brox, and O. Ronneberger, “3d u-net: learning dense volumetric segmentation from sparse annotation,” in *International conference on medical image computing and computer-assisted intervention*, pp. 424–432, Springer, 2016.
- [4] F. Milletari, N. Navab, and S.-A. Ahmadi, “V-net: Fully convolutional neural networks for volumetric medical image segmentation,” in *2016 fourth international conference on 3D vision (3DV)*, pp. 565–571, IEEE, 2016.
- [5] Jeya Maria Jose Valanarasu, Vishwanath A. Sindagi, Ilker Hacihaliloglu, Vishal M. Patel, “KiU-Net: Overcomplete Convolutional Architectures for Biomedical Image and Volumetric Segmentation” in *2020 MICCAI BraTS challenge*, MICCAI, 2020
- [6] Trace AP, Ortiz D, Deal A, Retrouvey M, Elzie C, Goodmurphy C, “Radiology’s Emerging Role in 3-D Printing Applications in Health Care” *J Am Coll Radiol*. Elsevier Inc; 2016; 13: 856–862.e4.
- [7] Rengier F, Mehndiratta A, Von Tengg-Kobligh H, Zechmann CM, Unterhinninghofen R, Kauczor HU, “3D printing based on imaging data: Review of medical applications” *Int J Comput Assist Radiol Surg*. 2010; 5: 335–341.

- [8] Aidan J. Cloonan, Danial Shahmirzadi, Danial Shahmirzadi, Barry J. Doyle, Elisa E. Konofagou, Tim M. McGloughlin, “3D-Printed Tissue-Mimicking Phantoms for Medical Imaging and Computational Validation Applications”
- [9] Thore M. Bücking, Emma R. Hill, James L. Robertson, Efthymios Maneas, Andrew A. Plumb, Daniil I. Nikitiche, “From medical imaging data to 3D printed anatomical models”
- [10] Autodesk Meshmixer [Internet]. [cited 1 Jan 2016]. Available: <http://www.meshmixer.com/>